HHS Public Access

Author manuscript

Mech Dev. Author manuscript; available in PMC 2018 February 01.

Published in final edited form as:

Mech Dev. 2017 February ; 143: 32–41. doi:10.1016/j.mod.2017.01.003.

Wnt signaling balances specification of the cardiac and pharyngeal muscle fields

Amrita Mandal[1,2], **Andrew Holowiecki**[1], **Yuntao Charlie Song**[1,2], and **Joshua S. Waxman**[1,*]

[1]Heart Institute, Molecular Cardiovascular Biology Division, Cincinnati Children's Hospital Medical Center, Cincinnati OH, USA

[2]Molecular and Developmental Biology Graduate Program, University of Cincinnati College of Medicine and Cincinnati Children's Hospital Medical Center, Cincinnati, OH 45208

Abstract

Canonical Wnt/β-catenin (Wnt) signaling plays multiple conserved roles during fate specification of cardiac progenitors in developing vertebrate embryos. Although lineage analysis in ascidians and mice has indicated there is a close relationship between the cardiac second heart field (SHF) and pharyngeal muscle (PM) progenitors, the signals underlying directional fate decisions of the cells within the cardio-pharyngeal muscle field in vertebrates are not yet understood. Here, we examined the temporal requirements of Wnt signaling in cardiac and PM development. In contrast to a previous report in chicken embryos that suggested Wnt inhibits PM development during somitogenesis, we find that in zebrafish embryos Wnt signaling is sufficient to repress PM development during anterior-posterior patterning. Importantly, the temporal sensitivity of dorso-anterior PMs to increased Wnt signaling largely overlaps with when Wnt signaling promotes specification of the adjacent cardiac progenitors. Furthermore, we find that excess early Wnt signaling can cell autonomously promote expansion of the first heart field (FHF) progenitors at the expense of PM and SHF within the anterior lateral plate mesoderm (ALPM). Our study provides insight into an antagonistic developmental mechanism that balances the sizes of the adjacent cardiac and PM progenitor fields in early vertebrate embryos.

Keywords

Wnt signaling; zebrafish; cardiac; pharyngeal muscle; mesoderm patterning; organ fields

Introduction

Organogenesis begins with commitment of multi-potent overlapping organ progenitor fields into a specific fate. During the course of development, cardiac and PM progenitors, the latter of which give rise to cranio-facial muscles, lay in close physical proximity in the ALPM and

*corresponding author: joshua.waxman@cchmc.org.

anterior paraxial mesoderm, respectively (Diogo et al., 2015; Nagelberg et al., 2015). Multiple developmental syndromes feature cardiac and cranio-facial defects (Diogo et al., 2015), with the most extensively studied being DiGeorge and velocardiofacial syndromes. Therefore, defects in signaling pathways that affect distinct or common cardio-pharyngeal progenitors may contribute to the molecular etiology of these syndromes.

Vertebrate heart development occurs in two waves. FHF progenitors differentiate earlier, primarily contributing to the left ventricle in mammals and birds and ~60% of the single ventricle and >90% of the atrium in the teleost zebrafish (Dyer and Kirby, 2009; Zhou et al., 2011). Later differentiating SHF progenitors contribute to growth of the heart through progressively adding to both poles of the heart. In mammals, the SHF contributes to the right ventricle, outflow tract and parts of the atria (Dyer and Kirby, 2009; Kelly, 2012; Zaffran and Kelly, 2012). In zebrafish, the SHF primarily contributes to the remaining 40% of ventricular cells (de Pater et al., 2009; Guner-Ataman et al., 2013; Zhou et al., 2011). A conserved aspect of vertebrate SHF progenitors is their ability to give rise to ventricular cardiomyocytes, endothelial cells, and smooth muscle of the outflow tract. In recent years, sophisticated retrospective clonal lineage tracing studies in mice have suggested there are also rare progenitors that give rise to both cardiac and PM, which fits with the close proximity of these progenitor fields within the anterior mesoderm (Lescroart et al., 2014; Lescroart et al., 2015; Lescroart et al., 2010).

Given the closeness of the cardiac and PM progenitor fields within the anterior mesoderm, which is exemplified by the existence of bi-potent cardio-pharyngeal progenitors, it is logical that there is significant overlap of genetic marker expression. In mice, the anterior mesoderm that harbors both SHF progenitors and PMs expresses markers including *Isl1, Tbx1*, and *Tcf21* (Harel et al., 2012; Nathan et al., 2008). Knockout mice reveal that *Isl1* and *Tbx1*, the latter of which is the primary gene associated with DiGeorge syndrome in humans (Baldini, 2002), are required to promote SHF and PM development (Harel et al., 2012; Nathan et al., 2008). Additionally, *Tcf21* KO mice also have cardiac outflow tract and PM defects, although less severe than Tbx1 (Harel et al., 2012). In zebrafish, while Isl1 does not have the broad role in SHF development that is found in mammals (de Pater et al., 2009), Tbx1 has a conserved role in cardiac and facial muscle development (Nevis et al., 2013; Piotrowski et al., 2003). A recent study in zebrafish has suggested that *tcf21* is expressed in ventricular OFT and PM progenitors (Nagelberg et al., 2015), although it was not determined if there are common cardiopharyngeal progenitors in zebrafish. Therefore, shared conserved genetic regulators promote the development of SHF cardiomyocytes and PM in vertebrates.

Common cardio-pharyngeal progenitors that give rise to the heart and atrial siphon muscles (ASMs) have been described in the tunicate *Ciona*, indicating the relationship of these progenitors may have originated early in the chordate lineage (Stolfi et al., 2010). Although analysis in vertebrates has identified signals that promote the generation of these progenitors, the comparably simple development of *Ciona* embryos has allowed for the detailed description of antagonistic relationships within cells of the SHF that generate the cardiac and ASMs. After secondary trunk ventral cells divide, differential gene expression within second heart precursors (SHPs) and ASM precursors determines their subsequent

fates as cardiac and ASM (Wang et al., 2013). Specifically, within the SHPs, NK4, the homolog of Nkx2.5 in vertebrates, inhibits Tbx1/10 expression, and promotes GATAa expression. Conversely, in the ASM precursors, Tbx1/10 promotes the muscle lineage through inhibition of GATAa expression. Thus, the simplicity of *Ciona* heart development has revealed a paradigm for antagonism between these conserved transcriptional signals within SHF lineages, which specifies the appropriate number of cardiac and PM progenitors.

In vertebrates, despite the conservation of molecular players, comparable mechanisms as found in *Ciona* that affect the fate decision to become cardiac or PM have not been described. Canonical Wnt signaling is a viable candidate as studies have indicated it plays important roles in the development of cardiac and PMs. Wnt signaling plays multiple developmental stage specific roles during cardiogenesis (Dohn and Waxman, 2012; Naito et al., 2006; Ueno et al., 2007). Prior to gastrulation, Wnt signaling promotes cardiac specification (Dohn and Waxman, 2012; Kwon et al., 2007; Naito et al., 2006; Paige et al., 2010; Ueno et al., 2007). At the end of gastrulation, Wnt inhibits cardiac differentiation (Dohn and Waxman, 2012; Ueno et al., 2007). Additionally, early Wnt signaling can promote cardiac fates at the expense of adjacent hematovascular progenitors (Liu et al., 2012; Naito et al., 2006; Sorrell et al., 2013). During later somitogenes in zebrafish, Wnt signaling can promote atrial differentiation (Dohn and Waxman, 2012). With respect to the role of Wnt signaling in PM development, however, there is currently a more limited understanding. Explant cultures and *in vivo* retrovirus injection in chicken embryos implicated canonical Wnt signaling from the dorsal neural tube and notochord as an inhibitor of PM. However, the conservation of this requirement for Wnt signaling has not been investigated (Tzahor et al., 2003).

In this study, we first sought to understand if there is a conserved requirement for Wnt in antagonizing PM development. Using transgenic heat-shock inducible lines to temporally manipulate Wnt signaling in zebrafish, we demonstrate that Wnt signaling primarily inhibits anterior PM development prior to gastrulation during anterior-posterior pattering, the developmental stage when it also promotes cardiac progenitor specification. Furthermore, excess Wnt signaling, through heat-shock induction of Wnt8a or co-depletion of the transcriptional repressors of Wnt signaling targets Tcf7la and Tcf7lb, promotes an expansion of the cardiac field into a region of the ALPM that typically harbors SHF and PM progenitors. Thus, Wnt signaling prior to gastrulation helps position the border between the FHF and the adjacent SHF and PM progenitor fields. Furthermore, blastula transplantation data suggests Wnt signaling cell autonomously promotes cardiac specification and inhibits PM development. Altogether, our study provides evidence that canonical Wnt signaling establishes the proportions of the adjacent cardiac and PM fields during early anterior-posterior patterning of mesoderm in vertebrates.

Results

Wnt signaling inhibits dorso-anterior PM development before gastrulation

Previous studies in chicken embryos have suggested that Wnt signaling from the dorsal neural tube inhibits PM development (Tzahor et al., 2003). However, the conservation of Wnt signaling in PM development has not been examined. To determine if, and when, Wnt

signaling is sufficient to inhibit PM development in zebrafish, we crossed hemizygous *Tg(hsp70l:wnt8a-GFP)* fish to homozygous *Tg(α-actin:GFP)* fish. The resulting embryos were heat-shocked to induce Wnt8a-GFP at the sphere (SP) stage (prior to gastrulation), tailbud (TB) stage (end of gastrulation), the 16 somite (s) stage (mid-somitogenesis), and 24 hours post-fertilization (hpf; end of somitogenesis). The transgenic embryos were sorted from their siblings that did not carry the heat-shock transgene using GFP fluorescence and the PMs were examined at 72 hpf when the majority of these muscles have differentiated (Schilling and Kimmel, 1997). We found that increased Wnt signaling prior to gastrulation promoted maximal loss of dorso-anterior head muscles. Specifically, increased Wnt signaling prior to gastrulation inhibited development of the EOMs, which are derived from the prechordal mesoderm, and the 1st and 2nd arch muscles (Fig. 1A, E). While ventral muscles of the first two arches were reduced, the dorsal muscles of these arches were lost (Fig. 1E). More posterior pharyngeal wall muscles (PWMs) were also reduced, while the somite-derived sternohyoideus (SH) was not overtly affected. The loss of dorso-anterior pharyngeal muscle correlated with a loss of *myod* expression, an indicator of skeletal muscle specification (Lin et al., 2006), at 32 hpf (Supplementary Material – Figure S1A,B). Wnt induction at the TB stage leads to comparatively less severe loss of dorso-anterior PMs (Fig. 1B, F), while induction at the 16s stage and 24 hpf appeared unaffected (Fig. 1C,D,G,H).

Tcf7l transcription factors are transcriptional repressors that are required to limit posteriorization of early Wnt signaling (Dorsky et al., 2003). To determine if endogenous Wnt signaling needs to be repressed to promote the PMs, we depleted Tcf7l1 proteins in the embryos using the previously validated *tcf7l1a* and *tcf7l1b* MOs (referred as Tcf7l1 depleted) that produce equivalent phenotypes to the mutants (Dorsky et al., 2003). Consistent with excess Wnt signaling prior to gastrulation, Tcf7l1 depleted embryos lost dorso-anterior PMs (Fig. 2A,B). Therefore, our data suggest that Wnt signaling is sufficient to inhibit PM development. However, in contrast to the analysis in chicken embryos that indicated a repressive role of Wnt signaling during somitogenesis, in zebrafish embryos the PMs are most sensitive to excess Wnt signaling prior to gastrulation.

Next, to determine if there is a requirement for Wnt signaling in PM development, hemizygous *Tg(hsp70l:dkk1-GFP)* fish were crossed to *Tg(α-actin:GFP)* fish. The resulting embryos were heat-shocked at SP, TB, 16s, and 24 hpf, sorted via GFP fluorescence, and examined as described above. As would be expected, inhibition of Wnt signaling before gastrulation produced embryos with larger heads due to anteriorization (Fig. 3A,E) (Lekven et al., 2001). Embryos were less sensitive to Wnt inhibition after the SP stage, with no overt changes in head size observed after heat-shock beginning at the TB stage (Fig. 3B–D,F–H). In contrast to the ostensible loss of muscles from excess Wnt signaling, it was difficult to assess if there was an increase in PM number, despite their overtly larger heads. However, there was an expansion of *myod* expression by 32 hpf within the head (Supplementary Material – Figure S1C,D). Furthermore, we counted muscle nuclei number in the AM muscle of embryos with decreased Wnt signaling prior to gastrulation and found that the muscles were composed of more cells (Fig. 4A–C). Although we attempted to analyze the requirement of the bicistronic *wnt8a* genes that are required to posteriorize the mesoderm, the embryos were not viable at 72 hpf and precluded analysis at this later stage. Together,

these results indicate Wnt signaling is necessary and sufficient to inhibit PM development prior to gastrulation when the organ progenitor fields are being established.

Wnt signaling limits anterior tcf21+ PM progenitors

Since we found that dorso-anterior PMs are most sensitive to perturbation of Wnt signaling during early patterning of the anterior-posterior axis, we wanted to understand the effects of Wnt signaling manipulation on distinct populations of the PM progenitors. A recent study demonstrated that *tcf21* marks PM progenitors that give rise to muscles in the zebrafish pharyngeal arches (1–7) (Nagelberg et al., 2015). Initially, the *tcf21+* cells comprise a single field within the ALPM (Fig. 5A–C) and are subsequently divided into two populations of *tcf21+* cells by 24 hpf (Fig. 5D–I) , with the anterior *tcf21+* population giving rise to the mandibular (1st) and hyoid (2nd) arches. Therefore, we predicted that the anterior *tcf21+* populations that give rise to the muscle within the 1st and 2nd pharyngeal arches would be lost or disrupted following changes in the levels of Wnt signaling. To examine the PM progenitor populations after manipulation of Wnt signaling, we depleted Tcf7l1 and Wnt8a from *Tg(tcf21:nucEGFP)* embryos. By the 14s stage, we found that depletion of Tcf7l1 proteins resulted in a slightly elongated field of *tcf21+* progenitors (Fig. 5A,B; Supplementary Material – Figure S2A,B). However, counting the *tcf21+* cells at the 14s stage, which is facilitated by the nuclear GFP, indicated there were actually decreased number of *tcf21+* progenitors in Tcf7l1 depleted embryos (Fig. 5J). By 24 hpf, a reduction in the anterior most population of *tcf21+* cells (we have designated field 1) was observed in Tcf7l1 depleted embryos (Fig. 5D,G,E,F,K). Conversely, inhibiting endogenous Wnt signaling via Wnt8a depletion led to an increased number of *tcf21+* cells at the 14s stage (Fig. 5J), despite reduced length of the single field (Fig. 5A,C; Supplementary Material – Figure S2A,C), coupled with an increase in the number of *tcf21+* cells within anterior field 1 at 24 hpf (Fig. 5D,G,F,I,K). Additionally, even though both field 1 and field 2 give rise to PMs in the 1st and 2nd arches (Nagelberg et al., 2015), manipulation of Wnt signaling did not affect the number of adjacent field 2 *tcf21+* cells at 24 hpf (Fig. 5K). Furthermore, the frequency in proliferation did not change between *tcf21+* populations (Supplementary Material – Figure S3) and there is only a minor increase in total *tcf21+* cells between these stages (Fig. 5J,K), supporting that the differences in *tcf21+* cell number after early Wnt manipulation are due to effects on cell specification. Taken together, our data suggest manipulation of Wnt signaling affects the number of cells in the anterior most *tcf21+* progenitor fields, which give rise to the dorso-anterior PMs in the 1st and 2nd arches.

Wnt signaling affects the overlap of nkx2.5 and tcf21 fields

Previous studies demonstrated that increased Wnt signaling prior to gastrulation, when it patterns the anterior-posterior axis, produces increased cardiac specification in zebrafish (Dohn and Waxman, 2012; Ueno et al., 2007). Therefore, we wanted to understand the relationship of the cardiac and PM progenitors after early Wnt signaling manipulation. We used the *Tg(nkx2.5:ZsYellow)* line to facilitate visualization of *nkx2.5+* cells, which primarily mark cardiac progenitors at mid-somitogenesis (Guner-Ataman et al., 2013), and the aforementioned heat-shock lines. Embryos were heat-shocked at the SP stage, as above, and we performed two-color in situ hybridization (ISH) with *tcf21* and *zsyellow* (*nkx2.5+* cells), in order to examine the relative effects on these populations within the ALPM at the

14s and 18s stages. At the 14s stage, the single *tcf21* expression domain overlaps posteriorly with *nkx2.5* (Fig. 6A,C). At the 18s stage, normally there is a small region of overlap with *nkx2.5* expression in the most anterior *tcf21*+ population ALPM (Fig. 6E,G), which has been reported previously (Nagelberg et al., 2015). Increasing Wnt signaling prior to gastrulation led to a dramatic expansion of *nkx2.5* expression into the *tcf21*+ pharyngeal field at the 14s and 18s stages (Fig. 6B,F). Conversely, decreasing Wnt signaling caused essentially no discernible overlap of *tcf21* and *nkx2.5* expression at the 14s stage (Fig. 6D), and minimal overlap of these populations at the 18s stage (Fig 6H).

To further examine the relationship between these markers within the ALPM, we depleted Tcf7l1 and Wnt8a proteins in *Tg(nkx2.5:zsyellow);Tg(tcf21:nucEGFP)* embryos and performed immunohistochemistry (IHC) at the 18s stage. Although the ALPM was not as affected as with Wnt induction, measuring the expression domains of these transgenic markers revealed that the overall length of the anterior *tcf21*+ progenitor domain was expanded at 18s in Tcf7l1 depleted embryos (Fig. 7A–C), consistent with what was observed at the 14s stage (Fig. 5A,B; Supplementary Material – Figure S2A,B). Furthermore, as with the ISH analysis of heat-shock Wnt induction, the overlap between *nkx2.5+* and *tcf21*+ progenitor populations within this domain was also expanded (Fig. 7A–C). Conversely, in Wnt8a depleted embryos, the overall anterior *tcf21+* population was minimally reduced in length, with the overlapping *tcf21+* and *nkx2.5+* domains also being reduced (Fig. 7D,E,F). Although not as striking, similar trends in overlap of these markers were also observed at the 14s stage (Supplementary Material – Figure S2A–C). Altogether, our data suggest that enhancing or reducing Wnt signaling prior to gastrulation changes the overlap between *nkx2.5+* and *tcf21+* domains within the ALPM.

While it is understood that Wnt signaling promotes cardiac specification prior to gastrulation (Dohn and Waxman, 2012; Ueno et al., 2007), the source of the surplus cardiac cells is not clear. Specifically, *nkx2.5+* cells give rise to both FHF and SHF-derived ventricular cardiomyocytes (George et al., 2015; Guner-Ataman et al., 2013). Additionally, a fate map of the ALPM in zebrafish has suggested that SHF progenitors lie anterior and medial to the FHF progenitors (Hami et al., 2011). Because anterior fates within the ALPM including the PM and hematovascular progenitors are lost (Sorrell et al., 2013), one possibility is that excess Wnt signaling promotes cardiomyocyte specification through differential effects on the FHF and SHF. Specifically, we hypothesized that early Wnt signaling may promote FHF specification at the expense of SHF. In order to determine if the SHF derivatives are affected by excess early Wnt signaling, we first performed *in situ* hybridization for *elastin b* (*elnb*), which is expressed in the smooth muscle cells of the OFT (Hami et al., 2011; Zhou et al., 2011), after heat-shock induction of Wnt8a-GFP at the SP stage. Interestingly, embryos with increased Wnt signaling prior to gastrulation had reduced or complete absence of *elnb+* cells (Fig. 8A–C). To further assay the effects on SHF progenitor markers after increased Wnt signaling, we used real-time quantitative PCR (RT-qPCR) for the SHF progenitor markers *mef2cb* and *ltbp3* at 24 hpf (Lazic and Scott, 2011; Zhou et al., 2011). At 24 hpf, when there was already increased FHF progenitor differentiation as indicated with *myl7* expression, there was a corresponding decrease in SHF progenitor expression (Fig. 8D). Altogether, our data suggest early Wnt signaling promotes an expansion of FHF progenitors at the expense of neighboring SHF and PM progenitors.

Wnt signaling acts cell-autonomously in PM progenitors

We next wanted to understand if Wnt signaling can act directly within PM progenitors or indirectly through affecting the surrounding environment to inhibit PM development. For instance, excess Wnt signaling prior to gastrulation also causes a merging of the anterior cardiac crest populations (Supplementary Material – Figure S3A,B) and loss of pharyngeal cartilage (Supplementary Material – Figure S4A,B). Thus, cranial skeletal muscle defects could be secondary to the neural crest derived cartilage defects or loss of the most anterior brain and eyes. To determine the cellular requirements of Wnt signaling, we performed blastula cell transplantation with Tcf7l1 depleted donor cells that were from embryos simultaneously carrying the *myl7:EGFP* and α-*actin:GFP* transgenes, which allowed unambiguous visualization of the differentiated CMs and PMs (Fig. 9A). After transplantation of cells at the SP stages, the frequency of donor cell contribution to heart and PMs, respectively, was assayed at 72 hpf (Fig. 9B,C). Consistent with what we have previously reported (Sorrell et al., 2013), when Tcf7l1 depleted donor cells were transplanted into the WT host embryos, we observed a significantly higher percentage of embryos with contribution to the cardiomyocyte lineage compared to WT donors transplanted into WT hosts. However, in the same set of experiments, the frequency of contribution to the PMs in embryos was significantly lower from Tcf7l1 depleted donor cells compared with WT donors transplanted to WT host embryos (Fig. 9D). One caveat of this experiment is that we rarely observed contribution to the dorsal 1st and 2nd arch muscles even from WT donor cells, suggesting these progenitors are a relatively rare population of cells. Overall, these results suggest Wnt signaling can cell autonomously repress PM development.

Discussion

In this study, we examined the role of Wnt signaling in allocating cardiac and PM cells during development. Using temporal activation and inhibition of Wnt signaling, as well as depletion of endogenous Wnt signaling ligand and transcriptional repressors, we found PM is most sensitive to manipulation of Wnt signaling prior to gastrulation in zebrafish. Increased Wnt signaling prior to gastrulation caused a severe reduction in anterior ventral 1st and 2nd arch muscles and loss of the dorsal 1st and 2nd arch muscles. Consistent with these phenotypes, increases and decreases in Wnt signaling reduce and expand, respectively, the most anterior *tcf21+* cell population, which harbors PM progenitors. The increased cardiomyocytes due to excess early Wnt signaling promotes FHF specification at the expense of the more anterior fates, which include the adjacent PM and SHF progenitors. Finally, blastula cell transplantation demonstrates that early cell autonomous Wnt signaling contributes to the generation of a proper number of PM cells.

Previous analysis of chick embryos has indicated that Wnt and BMP signaling from the neural tube inhibit PM development (Tzahor et al., 2003). Furthermore, a recent study indicated that endodermal BMP signaling promotes FGF signaling to control pharyngeal pouch development during early somitogenesis (Lovely et al., 2016), suggesting these signals may be expressed at an appropriate developmental time to function downstream of Wnt signaling in patterning PM progenitor cells. However, our analysis of BMP and FGF

ligands within zebrafish embryos after Wnt manipulation only revealed patterning defects that are consistent with early axis specification defects without effects on the pharyngeal pouches (Supplementary Material – Figure S6 and Figure S7). Thus, presently, our data do not support that Wnt is directly acting upon BMP and FGF signaling to establish the anterior PM field. Additionally, it has been proposed that inhibition of Wnt signaling via Frzb, which is expressed in the pharyngeal ectoderm of the 1st and 2nd arches, is sufficient to promote PM development in chick (Tzahor et al., 2003). Based on these previous results, which implicated a role for Wnt signaling during somitogenesis, when the neural tube and pharyngeal arches had formed in chick embryos, we expected to observe later requirements for Wnt signaling in PM development. Thus, we did not anticipate that PM development would be most sensitive to modulation of Wnt signaling prior to gastrulation during anterior-posterior patterning in zebrafish. Although we cannot rule out very subtle defects in the PMs, we did not find any evidence that PM development was perturbed when Wnt was manipulated after the end of gastrulation and throughout somitogenesis. Comparing the expression patterns of *frzb* in chicken and zebrafish embryos, zebrafish *frzb* is not expressed in cranial neural crest or 1st and 2nd pharyngeal arches during somitogenesis (zfin.org). Moreover, zebrafish *frzb* is expressed in the anterior pharyngeal arches. This expression begins around 2 days of development (zfin.org), significantly after the stages when we found Wnt signaling can affect PM development. Therefore, our results coupled with the lack of temporal conservation of *frzb* expression suggest that inhibit of Wnt signaling during somitogenesis is likely not a conserved requirement for early PM development in zebrafish.

Studies in mice have suggested there is a rare bi-potent pool of progenitors that can give rise to both SHF-derived cardiomyocytes and PMs (Lescroart et al., 2014; Lescroart et al., 2010). Based on the adjacent locations of cardiac and PM progenitors in the anterior lateral plate and paraxial mesoderm, it has been proposed that bi-potential progenitors that give rise to cardiac and PM may lie at this border (Diogo et al., 2015; Tzahor and Evans, 2011). Despite the close association of these progenitors and shared markers at later developmental stages, more recent lineage tracing studies using Confetti and MADM with Mesp1 inducible Cre-drivers indicate that cardiac FHF and SHF progenitors acquire their fates during gastrulation (Devine et al., 2014; Lescroart et al., 2015). Therefore, the proposed bi-potent cardio-pharyngeal progenitors may actually be specified at these early stages rather than at later stages. While our study does not directly address the existence of cardio-pharyngeal progenitors or when they emerge in zebrafish, our results highlight the closeness of these fields with the vertebrate anterior mesoderm. Furthermore, in line with the idea that mesodermal lineage potential is established very early during vertebrate development, our results indicate that patterning events mediated by Wnt signaling prior to gastrulation partition the adjacent cardiac and PM progenitors through inverse effects on their specification.

Our data indicate that Wnt signaling affects the fates of cardiac and PM progenitors as part of its role during anterior-posterior mesoderm patterning. However, it was counterintuitive that after an early increase in Wnt signaling the overlap of the anterior-most *tcf21+* and *nkx2.5+* progenitors was expanded in length, while decreasing early Wnt signaling had the opposite effect. The overlapping anterior-most *tcf21+* and *nkx2.5+* expressing cells within the ALPM give rise to the ventral 1st and 2nd arch muscles (Nagelberg et al., 2015).

Therefore, given the expansion of the *tcf21+/nkx2.5+* field after increased Wnt signaling prior to gastrulation, it is unexpected that these ventral PMs were actually overtly reduced, and not expanded. By comparison, the dorsal 1st and 2nd arch muscles are derived from the adjacent, more anterior progenitors that only express *tcf21* (Nagelberg et al., 2015). Thus, the loss of these dorsal PMs is consistent with posteriorization from excess early Wnt signaling and the reduction in cells making up the anterior most *tcf21+* progenitor field. Together, our data are consistent with the hypothesis that canonical Wnt signaling helps to define the border between the *tcf21+* and *tcf21+/nkx2.5+* progenitors within the anterior mesoderm.

Because we observe increased overlap of the *tcf21+* and *nkx2.5+* populations, not strictly an expansion of *nkx2.5* at the expense of *tcf21*, we speculate that excess canonical Wnt signaling must expand the expression of multiple genes that promote FHF cardiac potential, which overrides the developmental potential of ventral 1st and 2nd arch muscle progenitors. It is unlikely to be Nkx2.5 alone that confers this potential as a recent study indicated overexpression of Nkx2.5 does not promote cardiac specification (George et al., 2015). Another possible interpretation of our results could be that Wnt signaling promotes SHF-derived cardiac specification at the expense of PM and SHF-derived smooth muscles and endothelial cells. However, we think this interpretation is unlikely given expression of the established SHF progenitor markers is reduced after excess Wnt signaling prior to gastrulation. It is also feasible that some of the PM defects are secondary to neural crest-derived cartilage defects and loss of anterior head structures in embryos with increased Wnt signaling. However, the PM progenitors develop immediately anterior to the position of the midbrain hindbrain boundary, a region that is not lost in these embryos (Supplementary Material – Figure S6). Furthermore, our transplantation data suggest Wnt signaling can cell autonomously inhibit the development of PM muscle. Therefore, our data support that proper levels of Wnt signaling intrinsic to PM progenitors are necessary for their appropriate generation and the PM defects are likely not solely secondary to inappropriate anterior head development. Altogether, our results suggest that during anterior-posterior patterning canonical Wnt signaling directly promotes FHF specification at the expense of the adjacent more anterior hematovascular, PMs, and SHF cardiac progenitors.

In conclusion, our study provides insight into a previously unappreciated role of Wnt signaling in balancing cardiac and PM development of vertebrates. Our results indicate that at least in zebrafish the major inhibitory effects of Wnt signaling on PM development occur during anterior-posterior patterning of the mesoderm, which coincides with recent data supporting very early lineage restriction of mesodermal progenitors in mammals (Devine et al., 2014; Lescroart et al., 2014). Regulation of the molecular interface between FHF, SHF and PM specification is an exciting field open for further investigation. Knowledge of mechanisms that direct the fate choices of progenitors within the cardio-pharyngeal field is necessary to enhance our potential of preventing congenital syndromes with both cardiac and cranio-facial malformations.

Experimental Procedures

Zebrafish husbandry and transgenic lines

Zebrafish were raised and maintained following standard laboratory conditions (Westerfield, 1995). Transgenic lines used were: *Tg(hsp70l:wnt8a-GFP)*^{w34} (Weidinger et al., 2005) *Tg(hsp70l:dkk1-GFP)*^{w32} (Stoick-Cooper et al., 2007), *Tg(α-actin:GFP)* (Higashijima et al., 1997), *Tg(tcf21:nucEGFP)*^{pd41} *(Wang et al., 2011), TgBAC(−36nkx2.5:ZsYellow) (Zhou et al., 2011), Tg(−5.1myl7:EGFP)* ^{twu2} (Huang et al., 2003).

Heat-shock experiments and imaging of live embryos

For heat-shock experiments hemizygous *Tg(hsp70l:wnt8a-GFP)* and *Tg(hsp70l:dkk1-GFP)* were crossed with *Tg(α-actin-GFP), Tg(tcf21:nucEGFP) TgBAC(−36nkx2.5:ZsYellow)*, and *Tg(−5.1myl7:EGFP)* fish. Embryos were heat-shocked at 37°C for 30 min in a BioRad PCR machine. 1 hour post heat-shock GFP+ transgenic siblings were sorted from the GFP- siblings, which served as controls, using a Zeiss M2BioV12 Stereomicroscope. Embryos heat-shocked at early stages exhibited dorsalized and ventralized phenotypes upon Wnt modulation as described previously (Stoick-Cooper et al., 2007; Weidinger et al., 2005), which served as a confirmation that we are manipulating Wnt signaling in an expected manner. At 72 hpf, embryos were anesthetized with Tricaine (Sigma) and imaged with a Zeiss AxioImager with Apotome. To prevent pigmentation, 0.003% 1-phenyl-2-thiourea (PTU) treatment starting from 24 hpf was used.

Zebrafish morpholino (MO) oligonucleotide injection

Zebrafish embryos were injected at the one cell stage with a mixture of 3.5 ng *tcf7l1a* and 2.5 ng *tcf7l1b* MOs, as previously reported (Sorrell et al., 2013). *Wnt8a.1* and *wnt8a.2* MOs were injected at a dose of 2 ng of each (Lekven et al., 2001). For all MO injections, 1 ng of *p53* MO was co-injected to prevent non-specific induced cell death (Robu et al., 2007).

Whole mount immunohistochemistry, cell counting, and length measurements

Immunohistochemistry (IHC) was performed as described previously (Dohn and Waxman, 2012). The following antibodies were used: chicken anti-GFP primary antibody (1:250; Abcam), anti-chicken FITC secondary antibody (1:100; Southern Biotech), anti-RCFP rabbit polyclonal primary antibody (1:50; Clontech), anti-rabbit TRITC secondary antibody (1:200; Southern Biotech), anti-MHC monoclonal antibody (MF20) (1:10; Gift of D. Yelon), mouse monoclonal anti-pHH3 primary antibody (1:1000; Abcam), and goat anti-mouse Alexa Fluor 405 secondary antibody (1:100; Thermo Fisher). Embryos at 72 hpf were imaged using a Zeiss AxioImager with Apotome. To determine the number of *tcf21+* cells at 72 hpf, embryos were imaged with using a Zeiss AxioImager with Apotome and counted manually. To determine the number of *tcf21+/(GFP+)* progenitors and pHH3+ cells at the 14s stage and 24 hpf, after IHC was performed, embryos were mounted laterally on Ibidi μ-slides (cat #81501) and the GFP+ and pHH3+ expressing cells were imaged using a Nikon A1R inverted confocal microscope. Fluorescent nuclei and the overlay of marked cells from Z-stacks were then counted with the aid of Imaris software (Bitplane). To determine the overlap of *tcf21+* and *nkx2.5+* progenitors at the 18s stage, the embryos were mounted

dorsally and the different populations were imaged using a Zeiss AxioImager with Apotome. Measurement of the length of domains was performed using ImageJ. Statistical significance for cell counting and length measurements between two samples was assessed using Student's t-test with $p<0.05$ being considered statistically significant. Statistical significance for cell counting between more than two samples was assessed using a one-way ANOVA with $p<0.05$ being considered statistically significant.

In situ hybridization (ISH)

Single and two-color ISH were done as described previously (Lekven et al., 2001; Oxtoby and Jowett, 1993). All probes were reported previously: *tcf21* (ZDB-GENE-051113-88), *myod* (ZDB-GENE-980526-561), *dlx2a* (ZDB-GENE-980526-212), *elnb* (ZDB-GENE-061212-2), *fgf3* (ZDB-GENE-980526-178), *fgf8a* (ZDB-GENE-990415-72), *bmp2b* (ZDB-GENE-980526-474), *bmp4* (ZDB-GENE-980528-2059), and *zsyellow* (accession number: Q9U6Y4). INT-BCIP (Roche) and Fast red (Sigma) were used for two-color ISH. For images, embryo yolks were manually removed, the embryos were flat mounted and imaged using a Zeiss AxioImager2 compound microscope.

Quantitative real time PCR (RT-qPCR)

RT-qPCR was performed as described previously (D'Aniello et al., 2013). Briefly, total RNA was extracted from a pool of 30 whole embryos. Embryos were homogenized using Trizol (Ambion) and RNA was extracted using Purelink RNA Microkit (Invitrogen). 1ug of RNA was used to prepare cDNA using the ThermoScript Reverse Transcriptase kit (Invitrogen). PCR was performed in a BioRad CFX-96 PCR machine with Power SYBR Green PCR Master Mix (Applied Biosystems). Gene expression levels were standardized to β-actin and analyzed using the $2^{-\Delta\Delta CT}$ Livak Method and Student's *t*-test. *Myl7* and *ltbp3* primer sequences were described previously (D'Aniello et al., 2013) and (Zhou et al., 2011). Sequences for *mef2cb* primers are: F-ctatggaaaccaccgcaact and R-tgcgcagactgagagttgtt.

Blastula cell transplantation

For blastula cell transplantation, homozygous *Tg (myl7:EGFP)* and *Tg(α-actin:GFP)* adults were crossed. The resulting embryos were used as donors and injected at the one-cell stage with rhodamine-dextran lineage tracer along with the *tcf7l1* MOs. Approximately 30 cells from the control or *tcf7l1* depleted embryos were transplanted to the margin of control host blastula margin at SP stage. Embryos were raised and scored for CM and PM contribution at 48 and 72 hpf, respectively. The statistical significance of differences in the different populations was compared using a Chi-squared test with $p<0.05$ being considered statistically significant.

Alcian Blue staining

Alcian blue staining for cartilage was performed as previously described (Neuhauss et al., 1996)

Supplementary Material

Refer to Web version on PubMed Central for supplementary material.

Acknowledgments

The authors are grateful to A. Rydeen and J. Schumacher for comments on the manuscript. This research was supported by grants March of Dimes Grant 6-FY14-389 and NIH Grant R01 HL112893 to JSW.

References

Baldini A. DiGeorge syndrome: the use of model organisms to dissect complex genetics. Hum Mol Genet. 2002; 11:2363–2369. [PubMed: 12351571]

D'Aniello E, Rydeen AB, Anderson JL, Mandal A, Waxman JS. Depletion of Retinoic Acid Receptors Initiates a Novel Positive Feedback Mechanism that Promotes Teratogenic Increases in Retinoic Acid. PLoS genetics. 2013; 9:e1003689. [PubMed: 23990796]

de Pater E, Clijsters L, Marques SR, Lin YF, Garavito-Aguilar ZV, Yelon D, Bakkers J. Distinct phases of cardiomyocyte differentiation regulate growth of the zebrafish heart. Development. 2009; 136:1633–1641. [PubMed: 19395641]

Devine WP, Wythe JD, George M, Koshiba-Takeuchi K, Bruneau BG. Early patterning and specification of cardiac progenitors in gastrulating mesoderm. Elife. 2014:3.

Diogo R, Kelly RG, Christiaen L, Levine M, Ziermann JM, Molnar JL, Noden DM, Tzahor E. A new heart for a new head in vertebrate cardiopharyngeal evolution. Nature. 2015; 520:466–473. [PubMed: 25903628]

Dohn TE, Waxman JS. Distinct phases of Wnt/beta-catenin signaling direct cardiomyocyte formation in zebrafish. Developmental Biology. 2012; 361:364–376. [PubMed: 22094017]

Dorsky RI, Itoh M, Moon RT, Chitnis A. Two tcf3 genes cooperate to pattern the zebrafish brain. Development. 2003; 130:1937–1947. [PubMed: 12642497]

Dyer LA, Kirby ML. The role of secondary heart field in cardiac development. Dev Biol. 2009; 336:137–144. [PubMed: 19835857]

George V, Colombo S, Targoff KL. An early requirement for nkx2.5 ensures the first and second heart field ventricular identity and cardiac function into adulthood. Dev Biol. 2015; 400:10–22. [PubMed: 25536398]

Guner-Ataman B, Paffett-Lugassy N, Adams MS, Nevis KR, Jahangiri L, Obregon P, Kikuchi K, Poss KD, Burns CE, Burns CG. Zebrafish second heart field development relies on progenitor specification in anterior lateral plate mesoderm and nkx2.5 function. Development. 2013; 140:1353–1363. [PubMed: 23444361]

Hami D, Grimes AC, Tsai HJ, Kirby ML. Zebrafish cardiac development requires a conserved secondary heart field. Development. 2011; 138:2389–2398. [PubMed: 21558385]

Harel I, Maezawa Y, Avraham R, Rinon A, Ma HY, Cross JW, Leviatan N, Hegesh J, Roy A, Jacob-Hirsch J, Rechavi G, Carvajal J, Tole S, Kioussi C, Quaggin S, Tzahor E. Pharyngeal mesoderm regulatory network controls cardiac and head muscle morphogenesis. Proceedings of the National Academy of Sciences of the United States of America. 2012; 109:18839–18844. [PubMed: 23112163]

Higashijima S, Okamoto H, Ueno N, Hotta Y, Eguchi G. High-frequency generation of transgenic zebrafish which reliably express GFP in whole muscles or the whole body by using promoters of zebrafish origin. Dev Biol. 1997; 192:289–299. [PubMed: 9441668]

Huang CJ, Tu CT, Hsiao CD, Hsieh FJ, Tsai HJ. Germ-line transmission of a myocardium-specific GFP transgene reveals critical regulatory elements in the cardiac myosin light chain 2 promoter of zebrafish. Developmental dynamics : an official publication of the American Association of Anatomists. 2003; 228:30–40. [PubMed: 12950077]

Kelly RG. The second heart field. Curr Top Dev Biol. 2012; 100:33–65. [PubMed: 22449840]

Kwon C, Arnold J, Hsiao EC, Taketo MM, Conklin BR, Srivastava D. Canonical Wnt signaling is a positive regulator of mammalian cardiac progenitors. Proc Natl Acad Sci U S A. 2007; 104:10894–10899. [PubMed: 17576928]

Lazic S, Scott IC. Mef2cb regulates late myocardial cell addition from a second heart field-like population of progenitors in zebrafish. Dev Biol. 2011; 354:123–133. [PubMed: 21466801]

Lekven AC, Thorpe CJ, Waxman JS, Moon RT. Zebrafish wnt8 encodes two wnt8 proteins on a bicistronic transcript and is required for mesoderm and neurectoderm patterning. Dev Cell. 2001; 1:103–114. [PubMed: 11703928]

Lescroart F, Chabab S, Lin X, Rulands S, Paulissen C, Rodolosse A, Auer H, Achouri Y, Dubois C, Bondue A, Simons BD, Blanpain C. Early lineage restriction in temporally distinct populations of Mesp1 progenitors during mammalian heart development. Nat Cell Biol. 2014; 16:829–840. [PubMed: 25150979]

Lescroart F, Hamou W, Francou A, Theveniau-Ruissy M, Kelly RG, Buckingham M. Clonal analysis reveals a common origin between nonsomite-derived neck muscles and heart myocardium. Proc Natl Acad Sci U S A. 2015; 112:1446–1451. [PubMed: 25605943]

Lescroart F, Kelly RG, Le Garrec JF, Nicolas JF, Meilhac SM, Buckingham M. Clonal analysis reveals common lineage relationships between head muscles and second heart field derivatives in the mouse embryo. Development. 2010; 137:3269–3279. [PubMed: 20823066]

Lin CY, Yung RF, Lee HC, Chen WT, Chen YH, Tsai HJ. Myogenic regulatory factors Myf5 and Myod function distinctly during craniofacial myogenesis of zebrafish. Dev Biol. 2006; 299:594–608. [PubMed: 17007832]

Liu F, Kang I, Park C, Chang LW, Wang W, Lee D, Lim DS, Vittet D, Nerbonne JM, Choi K. ER71 specifies Flk-1+ hemangiogenic mesoderm by inhibiting cardiac mesoderm and Wnt signaling. Blood. 2012

Lovely CB, Swartz ME, McCarthy N, Norrie JL, Eberhart JK. Bmp signaling mediates endoderm pouch morphogenesis by regulating Fgf signaling in zebrafish. Development. 2016; 143:2000–2011. [PubMed: 27122171]

Nagelberg D, Wang J, Su R, Torres-Vazquez J, Targoff KL, Poss KD, Knaut H. Origin, Specification, and Plasticity of the Great Vessels of the Heart. Curr Biol. 2015; 25:2099–2110. [PubMed: 26255850]

Naito AT, Shiojima I, Akazawa H, Hidaka K, Morisaki T, Kikuchi A, Komuro I. Developmental stage-specific biphasic roles of Wnt/beta-catenin signaling in cardiomyogenesis and hematopoiesis. Proc Natl Acad Sci U S A. 2006; 103:19812–19817. [PubMed: 17170140]

Nathan E, Monovich A, Tirosh-Finkel L, Harrelson Z, Rousso T, Rinon A, Harel I, Evans SM, Tzahor E. The contribution of Islet1-expressing splanchnic mesoderm cells to distinct branchiomeric muscles reveals significant heterogeneity in head muscle development. Development. 2008; 135:647–657. [PubMed: 18184728]

Neuhauss SC, Solnica-Krezel L, Schier AF, Zwartkruis F, Stemple DL, Malicki J, Abdelilah S, Stainier DY, Driever W. Mutations affecting craniofacial development in zebrafish. Development. 1996; 123:357–367. [PubMed: 9007255]

Nevis K, Obregon P, Walsh C, Guner-Ataman B, Burns CG, Burns CE. Tbx1 is required for second heart field proliferation in zebrafish. Dev Dyn. 2013; 242:550–559. [PubMed: 23335360]

Oxtoby E, Jowett T. Cloning of the zebrafish krox-20 gene (krx-20) and its expression during hindbrain development. Nucleic Acids Res. 1993; 21:1087–1095. [PubMed: 8464695]

Paige SL, Osugi T, Afanasiev OK, Pabon L, Reinecke H, Murry CE. Endogenous Wnt/beta-catenin signaling is required for cardiac differentiation in human embryonic stem cells. PLoS One. 2010; 5:e11134. [PubMed: 20559569]

Piotrowski T, Ahn DG, Schilling TF, Nair S, Ruvinsky I, Geisler R, Rauch GJ, Haffter P, Zon LI, Zhou Y, Foott H, Dawid IB, Ho RK. The zebrafish van gogh mutation disrupts tbx1, which is involved in the DiGeorge deletion syndrome in humans. Development. 2003; 130:5043–5052. [PubMed: 12952905]

Robu ME, Larson JD, Nasevicius A, Beiraghi S, Brenner C, Farber SA, Ekker SC. p53 activation by knockdown technologies. PLoS genetics. 2007; 3:e78. [PubMed: 17530925]

Schilling TF, Kimmel CB. Musculoskeletal patterning in the pharyngeal segments of the zebrafish embryo. Development. 1997; 124:2945–2960. [PubMed: 9247337]

Sorrell MR, Dohn TE, D'Aniello E, Waxman JS. Tcf7l1 proteins cell autonomously restrict cardiomyocyte and promote endothelial specification in zebrafish. Developmental Biology. 2013

Stoick-Cooper CL, Weidinger G, Riehle KJ, Hubbert C, Major MB, Fausto N, Moon RT. Distinct Wnt signaling pathways have opposing roles in appendage regeneration. Development. 2007; 134:479–489. [PubMed: 17185322]

Stolfi A, Gainous TB, Young JJ, Mori A, Levine M, Christiaen L. Early chordate origins of the vertebrate second heart field. Science. 2010; 329:565–568. [PubMed: 20671188]

Tzahor E, Evans SM. Pharyngeal mesoderm development during embryogenesis: implications for both heart and head myogenesis. Cardiovascular Research. 2011; 91:196–202. [PubMed: 21498416]

Tzahor E, Kempf H, Mootoosamy RC, Poon AC, Abzhanov A, Tabin CJ, Dietrich S, Lassar AB. Antagonists of Wnt and BMP signaling promote the formation of vertebrate head muscle. Genes Dev. 2003; 17:3087–3099. [PubMed: 14701876]

Ueno S, Weidinger G, Osugi T, Kohn AD, Golob JL, Pabon L, Reinecke H, Moon RT, Murry CE. Biphasic role for Wnt/beta-catenin signaling in cardiac specification in zebrafish and embryonic stem cells. Proc Natl Acad Sci U S A. 2007; 104:9685–9690. [PubMed: 17522258]

Wang J, Panakova D, Kikuchi K, Holdway JE, Gemberling M, Burris JS, Singh SP, Dickson AL, Lin YF, Sabeh MK, Werdich AA, Yelon D, Macrae CA, Poss KD. The regenerative capacity of zebrafish reverses cardiac failure caused by genetic cardiomyocyte depletion. Development. 2011; 138:3421–3430. [PubMed: 21752928]

Wang W, Razy-Krajka F, Siu E, Ketcham A, Christiaen L. NK4 antagonizes Tbx1/10 to promote cardiac versus pharyngeal muscle fate in the ascidian second heart field. PLoS Biol. 2013; 11:e1001725. [PubMed: 24311985]

Weidinger G, Thorpe CJ, Wuennenberg-Stapleton K, Ngai J, Moon RT. The Sp1-related transcription factors sp5 and sp5-like act downstream of Wnt/beta-catenin signaling in mesoderm and neuroectoderm patterning. Curr Biol. 2005; 15:489–500. [PubMed: 15797017]

Westerfield, M. The Zebrafish Book: A guide for the labratory use of zebrafish (Danio rerio). 3. University of Oregon Press; 1995.

Zaffran S, Kelly RG. New developments in the second heart field. Differentiation. 2012; 84:17–24. [PubMed: 22521611]

Zhou Y, Cashman TJ, Nevis KR, Obregon P, Carney SA, Liu Y, Gu A, Mosimann C, Sondalle S, Peterson RE, Heideman W, Burns CE, Burns CG. Latent TGF-beta binding protein 3 identifies a second heart field in zebrafish. Nature. 2011; 474:645–648. [PubMed: 21623370]

Highlights

- Wnt signaling inhibits pharyngeal muscle development prior to gastrulation
- Wnt signaling expands the first heart field at the expense of pharyngeal muscle
- Wnt signaling inhibits second heart field development
- Wnt signaling cell autonomously inhibits pharyngeal muscle development

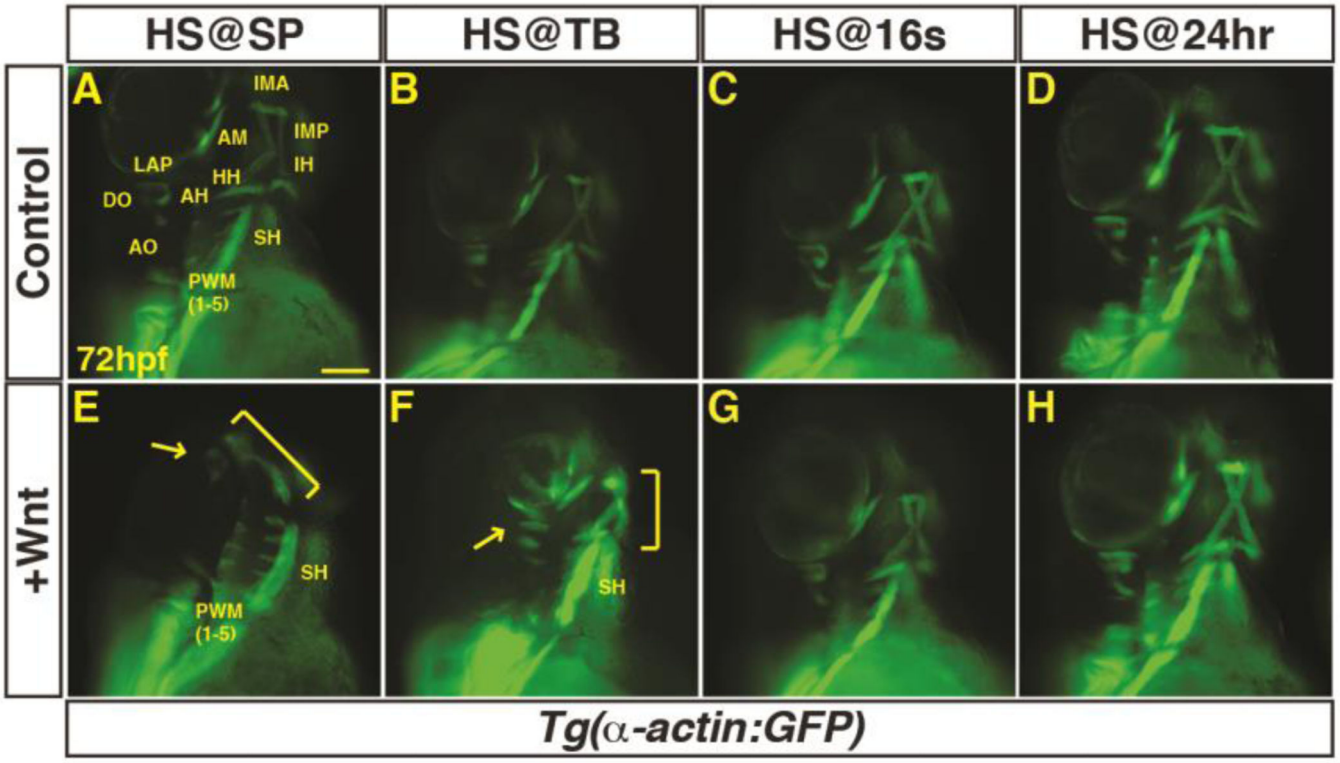

Figure 1. Excess Wnt signaling inhibits PM development during gastrulation

(A–P) *Tg(α-actin:GFP)* control sibling embryos and embryos with increased Wnt signaling (*hsp70l:wnt8a-GFP+*). (A,E) After increasing Wnt signaling from heat-shock (HS) at the SP stage, the EOMs, dorsal 1st and 2nd arch PMs are lost (arrow), while the ventral 1st and 2nd arch PMs are reduced (bracket). PW muscles are also reduced, while the SH was overtly unaffected. (B,F) After increasing Wnt signaling at the TB stage, there is a similar but less severe loss of EOMs, 1st and 2nd arch PMs (dorsal PMs - arrow; ventral PMs bracket). (C, G, D, H) Wnt signaling does not overtly affect PM development at later stages. Muscle nomenclature used is from (Schilling and Kimmel, 1997). 1st arch muscles - intermandibularis anterior (IMA), intermandibularis posterior (IMP), adductor mandibulae (AM), levator arcus palatine (LAP), dilatator opercula (DO). 2nd (hyoid) arch muscles - hyohyal (HH), interhyal (IH), adductor hyomandibulae (AH), adductor opercula (AO), and levator opercula (LO). Embryos are at 72 hpf. Images are anterior ventrolateral views. Anterior is up in all images. Heat-shock (HS). >15 embryos were examined for each condition. Scale bar indicates 100 μm.

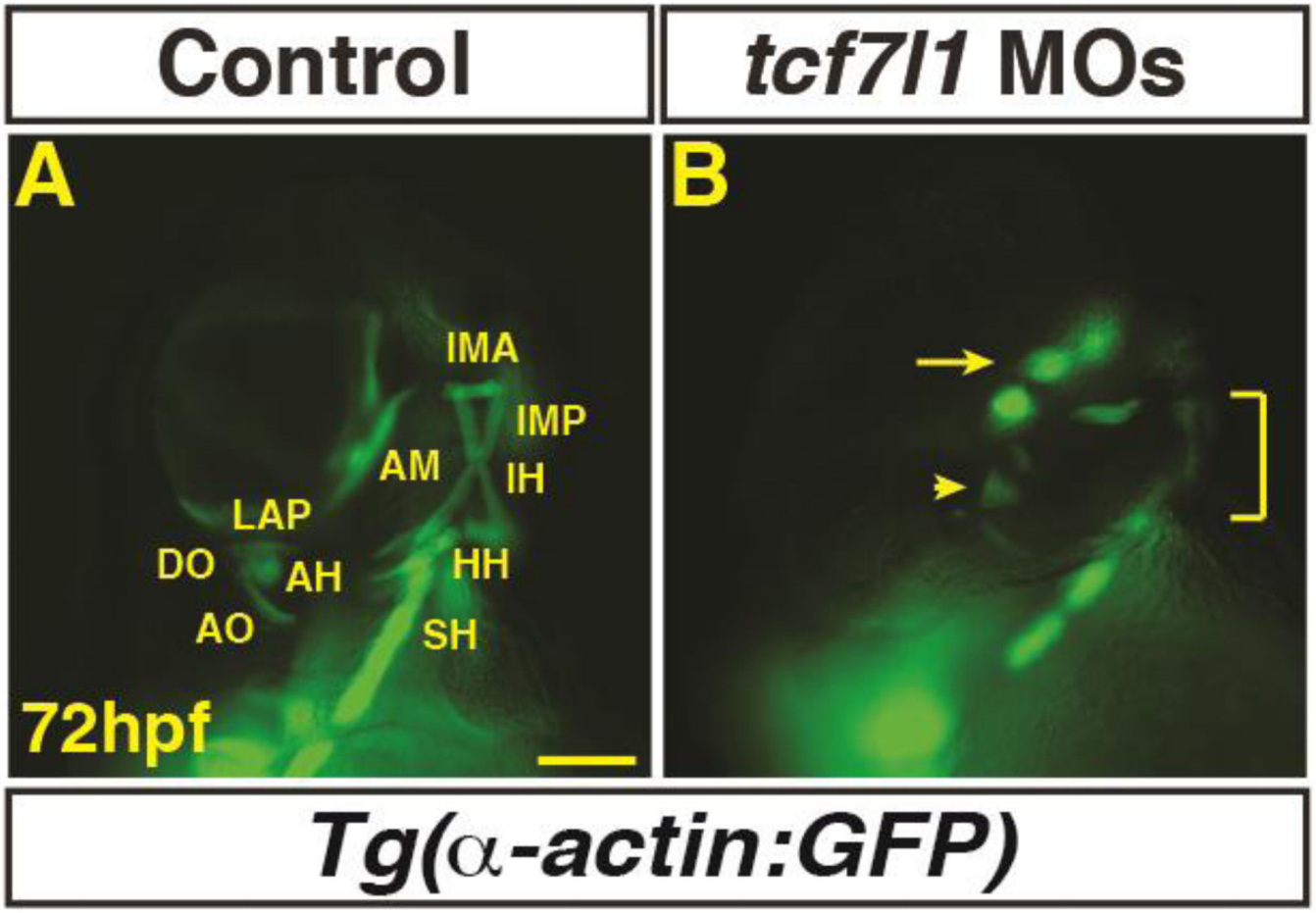

Figure 2. Tcf7l1 depletion causes loss of dorso-anterior PMs

(A–B) Control and Tcf7l1 depleted *Tg(α-actin:GFP)* embryos at 72 hpf. Tcf7l1 depletion resulted in similar loss of dorso-anterior PMs as increasing Wnt signaling prior to gastrulation. EOMs (arrow), 1st and 2nd PMs are severely reduced and misorganized or lost (arrowhead). Ventral 1st and 2nd arch muscles are reduced (bracket). Views are anterior ventrolateral. >15 embryos were examined for each condition. Scale bar indicates 100 μm.

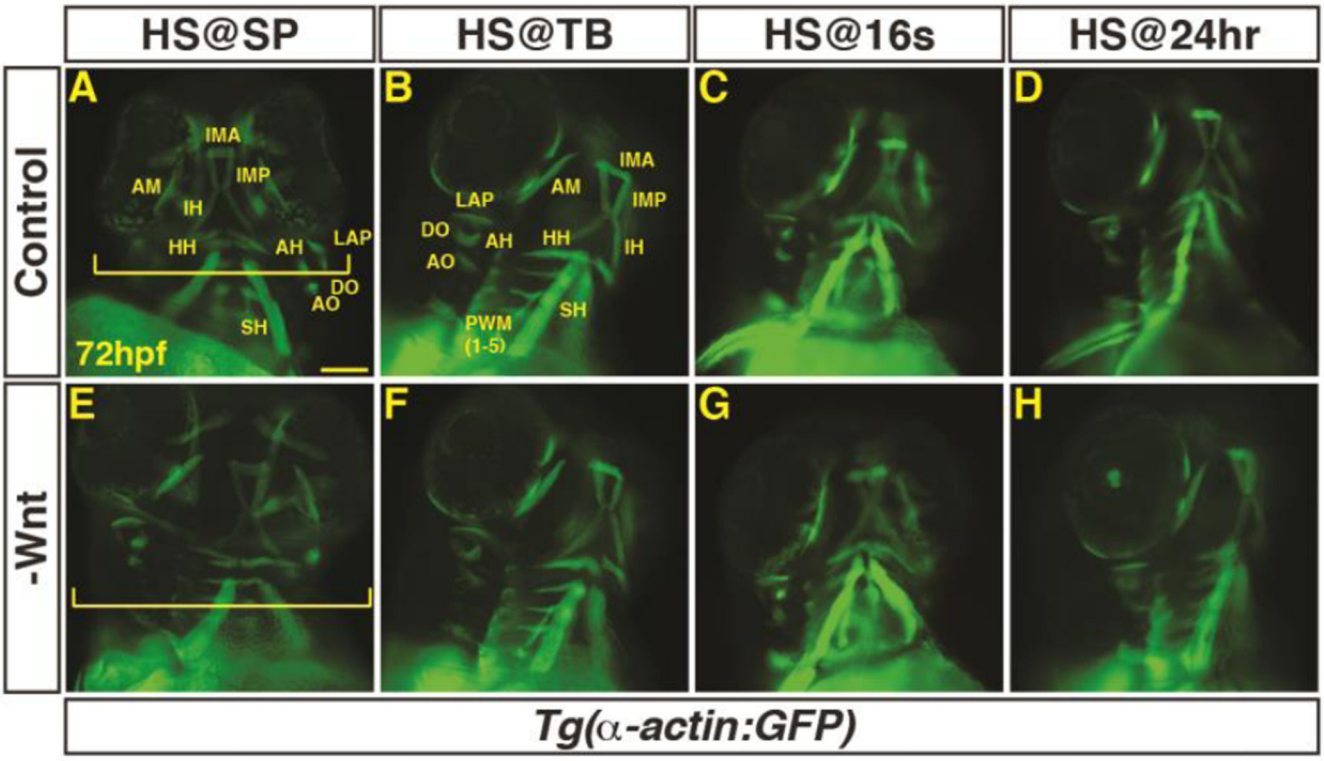

Figure 3. Decreased Wnt signaling during gastrulation increases head size with minimal effect on PM morphology

(A–H) *Tg(α-actin:GFP)* control sibling embryos and embryos with decreased Wnt signaling (*hsp70l:dkk1-GFP+)*. (A,E) After decreasing Wnt signaling at the SP stage, the embryos have enlarged heads (brackets). (B–D, F–H) After decreasing Wnt signaling at later stages, there was no discernible effect on pharyngeal muscles. Embryos are at 72 hpf. Images in A,E are anterior ventral views. Images in B–D, F–H are anterior ventro-lateral views. Anterior is up in all images. Heat-shock (HS). >15 embryos were examined for each condition. Scale bar indicates 100 μm.

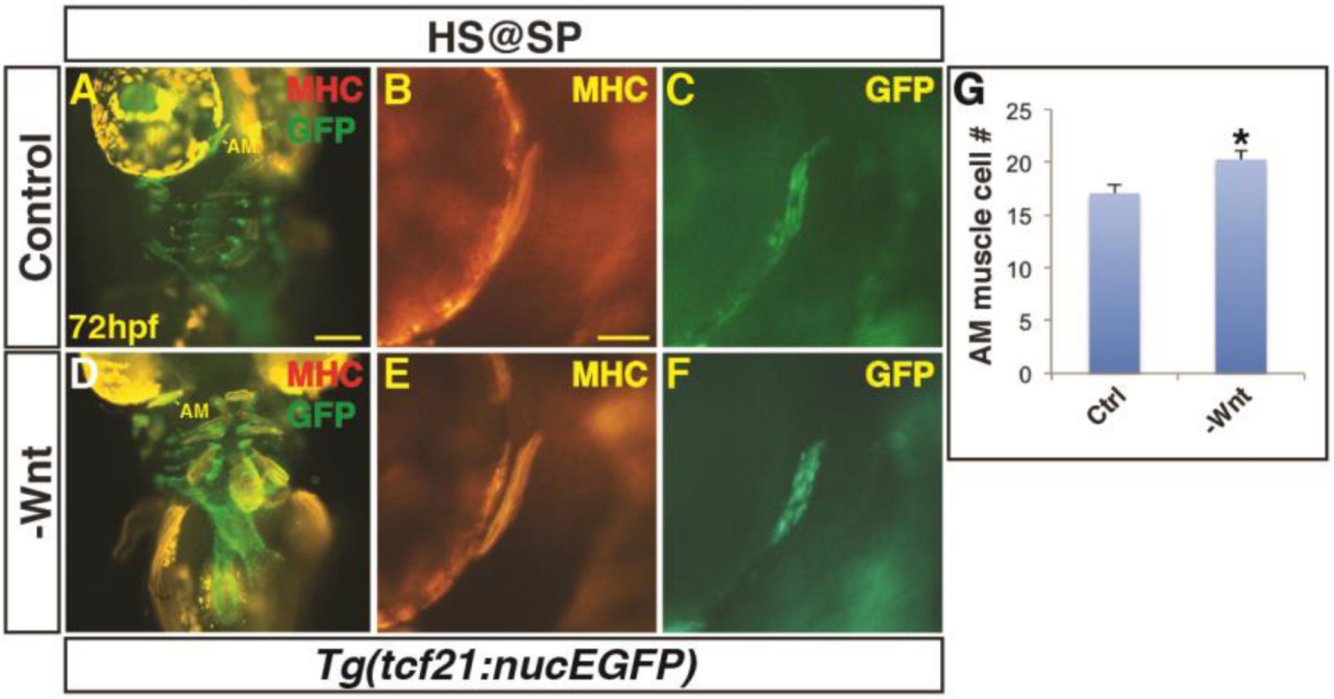

Figure 4. Decreased Wnt signaling causes an increase in 1st arch PM cells

(A, B) *Tg(tcf21:nucEGFP)* control sibling embryos and embryos with decreased Wnt signaling at the SP stage. Decreased Wnt signaling causes enlargement of the 1st arch AM muscle (boxes). Sarcomeric myosin (MHC; red). NucGFP (green). (B, E) MHC alone of AM muscles. (C, F) NucEGFP alone of AM. (G) Graph depicting quantification of nuclei in the AM muscles. Decreasing Wnt signaling at the SP stage produces a modest, but significant increase in AM muscle nuclei. Control embryos n=15, *Tg(hsp70l:dkk1-GFP)* embryos n=7. Asterisks in all graphs indicate $p<0.05$. Error bars in all graphs indicate S.E.M. Scale bar in A indicates 100 μm. Scale bar in B indicates 50 μm.

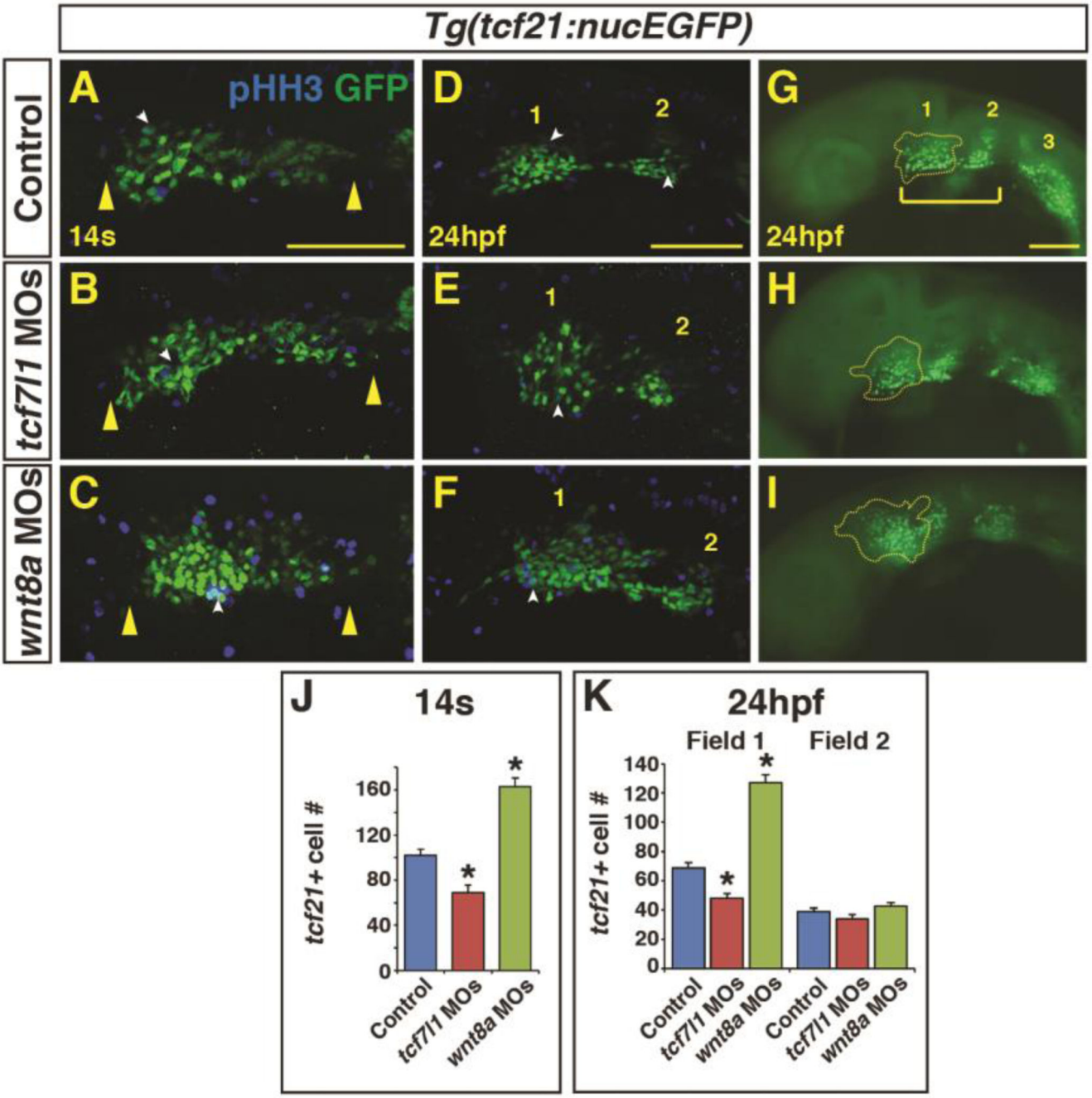

Figure 5. Endogenous Wnt signaling components restrict *tcf21+* PM progenitor development

(A–C) *Tcf21+* (GFP+) cells within the ALPM of *Tg(tcf21:nucEGFP)* control, Tcf7l1 depleted, and Wnt8a depleted embryos at the 14s stage. Images are dorsal views of the left side of the embryos with anterior left. Yellow arrowheads indicate size of field. (D-I) *Tcf21+* (GFP+) cells within the ALPM of *Tg(tcf21:nucEGFP)* control, Tcf7l1 depleted, and Wnt8a depleted embryos at 24 hpf. Images are lateral views with anterior left. (E,H) Tcf7l1 depletion produces a loss of the anterior most *tcf21+* progenitors (yellow outline). (F,I) Wnt8a depletion results in expansion of the anterior most pharyngeal *tcf21+* progenitors.

White arrowheads in A-F indicate overlap between GFP+ and phospho-histone H3 (pHH3)+ cells (see Supplementary Material – Figure S3 for analysis of pHH3). Bracket in G indicates the anterior *tcf21+* field of cells that give rise to the 1st and 2nd arch muscles. Numbers 1 and 2 in D-G indicate the two anterior *tcf21+* fields of cells. Number 3 in G indicates the more posterior *tcf21+* population that gives rise to PM in arches 3–7 (Nagelberg et al., 2015). Images A-F are confocal images. (J) Graph depicting quantification *of tcf21+* progenitors at the 14s stage. *Tg(tcf21:nucEGFP)* control n=15, Tcf7l1 depleted n=10, and Wnt8a depleted embryos n=10. (K) Graph depicting quantification of *tcf21+* progenitors at the 24hpf. *Tg(tcf21:nucEGFP)* control n=10, Tcf7l1 depleted n=13, and Wnt8a depleted embryos n=10. Cell counts are from confocal images of the *tcf21+* field on one side of the embryo. There is a significant decrease in *tcf21+* progenitors with Tcf7l1 depletion and conversely a significant increase in *tcf21+* progenitors following Wnt8a depletion in the total field at the 14s stage and anterior field at 24 hpf. Scale bars indicates 100 μm.

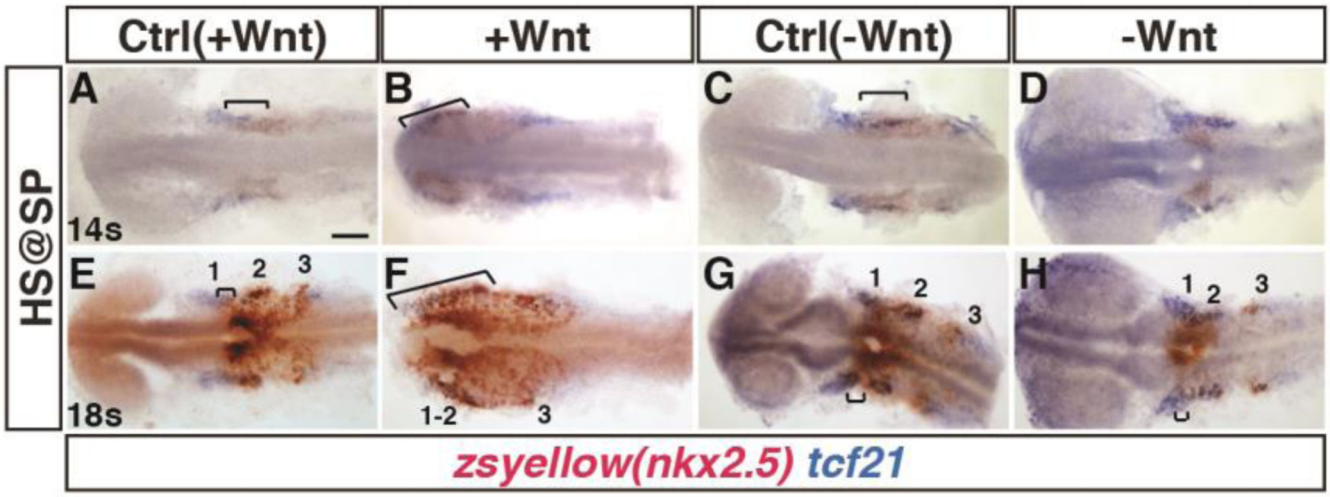

Figure 6. Manipulation of Wnt signaling affects the overlap of *nkx2.5+* and *tcf21+* domains within the ALPM

(A–H) *Tg(nkx2.5:ZsYellow)* control sibling embryos and embryos with increased and decreased Wnt signaling at the SP stage. (A,B,E,F) Two-color ISH of *zsyellow (nkx2.5;* brownish red) and *tcf21* (blue) at the 14s and 18s stages shows expansion of the lateral *nkx2.5+* domains into the anterior *tcf21+* domain after increased Wnt signaling. Numbers in E indicate the three *tcf21+* fields depicted in Figure 5. (C,D,G,H) Decreasing Wnt signaling prior to gastrulation causes a decrease in the overlap of *nkx2.5* and *tcf21* at the 14s and 18s stages. Significant overlap between *nkx2.5* and *tcf21* could not be detected at the 14s stage in embryos when with Wnt signaling was inhibited prior to gastrulaiton. Images are dorsal views with anterior to left. Brackets indicate overlap of *nkx2.5+* and *tcf21+* domains. For each group >15 embryos were examined. Scale bar indicates 100 μm.

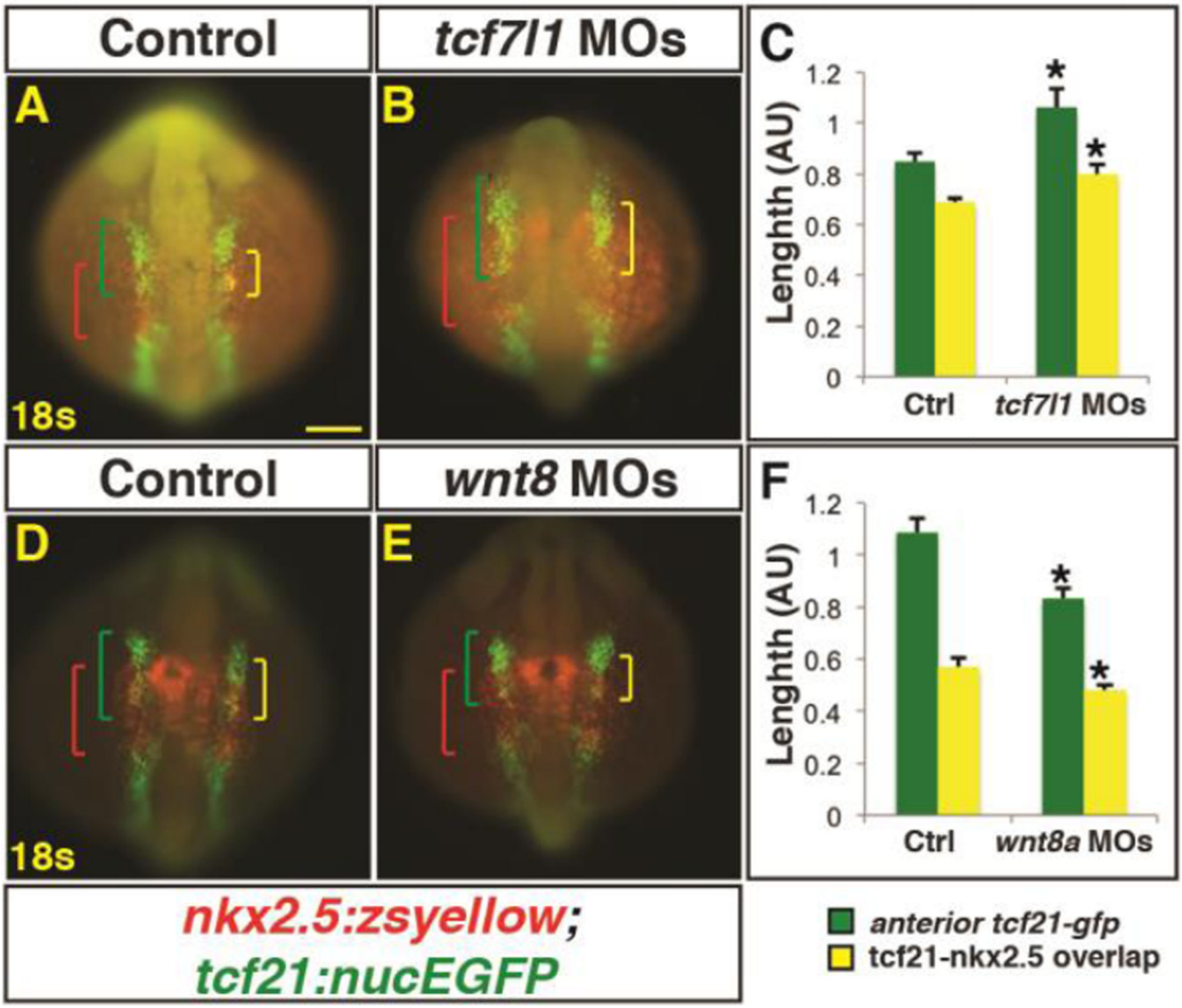

Figure 7. Manipulation of endogenous Wnt signaling affects the size of the *nkx2.5+* and *tcf21+* domains

(A,B,D,E) *Tg(nkx2.5:ZsYellow);Tg(tcf21:nucEGFP)* control, Tcf7l1 depleted, and Wnt8a depleted embryos at the 18s stage. Tcf7l1 depletion expands the total anterior *tcf21+* progenitor domain length (green brackets) as well as the overlapping expression (yellow brackets) within the ALPM. (C) Graph depicting measurements of the total *tcf21+* progenitors and overlap with *nkx2.5+* progenitors from Tcf7l1 depleted embryos. Control embryos n=10, Tcf7l1 depleted embryos n=9. (D, E) Wnt8a depletion reduces the overall length of the *tcf21+* domain and the overlap with the *nkx2.5+* progenitor domain. (F) Graph depicting measurements of the total *tcf21+* progenitors and overlap with *nkx2.5+* progenitors from Wnt8a depleted embryos. Control embryos n=8, Wnt8a depleted embryos n=10. Green brackets - anterior *tcf21+* progenitors. Red brackets - *nkx2.5+* progenitors. Yellow brackets - regions of overlap between *tcf21+* and *nkx2.5+* domains. Scale bar indicates 100 μm.

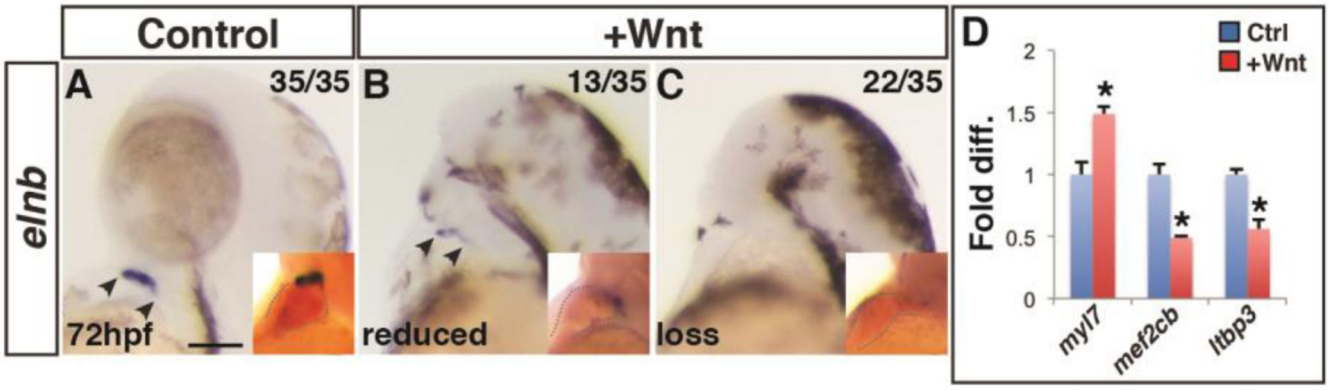

Figure 8. Increased Wnt signaling promotes loss of the SHF

(A–C) Control sibling embryos and embryos after increased Wnt signaling at the SP stage. Increasing Wnt signaling prior to gastrulation leads to loss of the SHF-derived OFT smooth muscle (*elnb*). Inserts indicate embryos with two-color ISH for *myl7* and *elnb*. Outlines indicate the hearts. (D) RT-qPCR for cardiac differentiation and SHF progenitor marker expression at 24 hpf. Increasing Wnt signaling prior to gastrulation promotes increased expression of the pan-cardiac differentiation marker *myl7* and decreased expression of the SHF markers *mef2cb* and *ltbp3* compared to WT sibling controls. Images are lateral views with anterior upward. Scale bar indicates 100 μm.

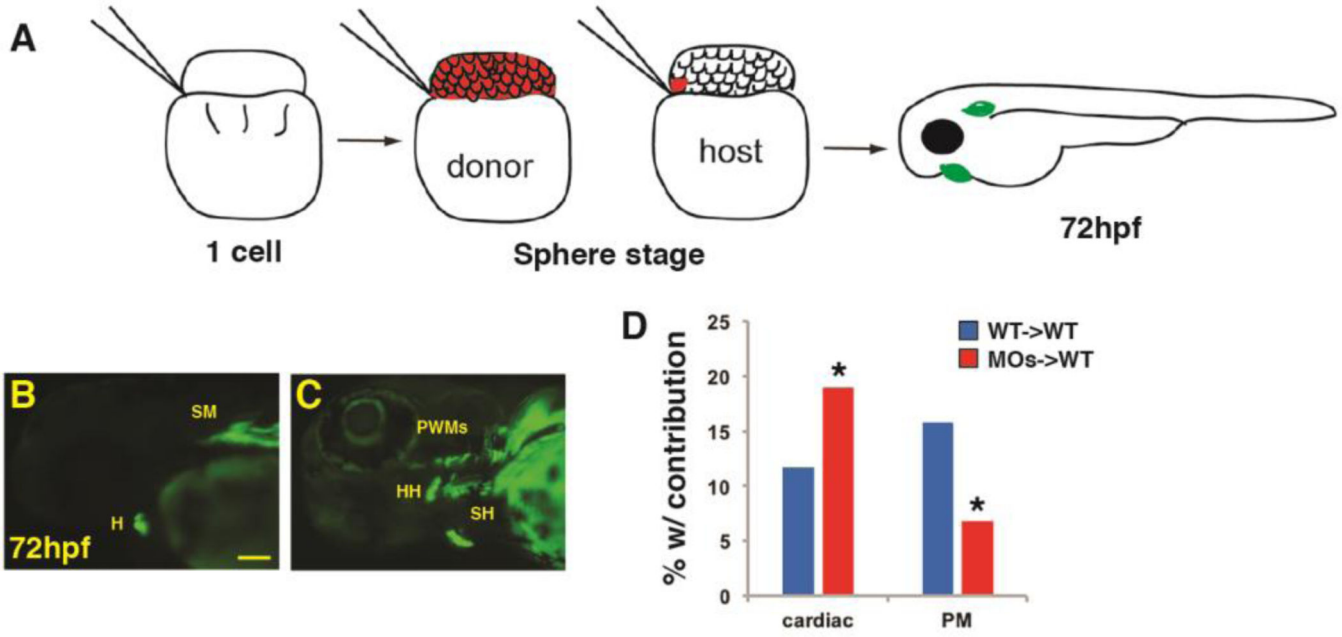

Figure 9. Wnt signaling cell-autonomously inhibits PM specification

(A) Schematic of blastula cell transplantation method. (B, C) Representative donor cells that incorporated into the heart and PMs at 72 hpf. (D) Graph indicating the frequency of donor cell contribution in embryos to the heart and the PMs. WT donor cells ->WT host transplants n=240. Tcf7l depleted donor cells ->WT host em bryos n=221. Tcf7l1 depleted donor cells contributed significantly more to the cardiomyocytes and less frequently to the PMs compared to WT donors. Images are lateral views with anterior leftwards. Scale bar indicates 100 μm.